Supplementary Materials for

Superflexible C_{68}-graphyne as promising anode materials for lithium-ion batteries

Bozhao Wu[1], Xiangzheng Jia[1], Yanlei Wang[2], Jinxi Hu[1], Enlai Gao[1*] and Ze Liu[1*]

[1]Department of Engineering Mechanics, School of Civil Engineering, Wuhan University, Wuhan, Hubei 430072, China.

[2]Beijing Key Laboratory of Ionic Liquids Clean Process, CAS Key Laboratory of Green Process and Engineering, Institute of Process Engineering, Chinese Academy of Sciences, Beijing 100190, China.

[*]Corresponding authors. Email: enlaigao@whu.edu.cn; ze.liu@whu.edu.cn

The Supporting Materials contain

- Supplementary Figures S1-S9.
- Supplementary Tables S1-S2.

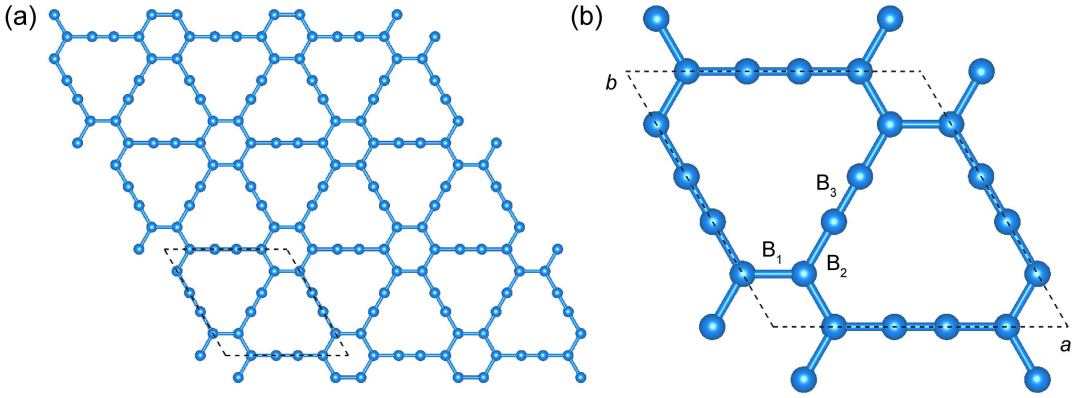

Fig. S1 (a) Schematic diagram of γ-GY and (b) its primitive cell, different bonds are marked as $B_{1\text{-}3}$.

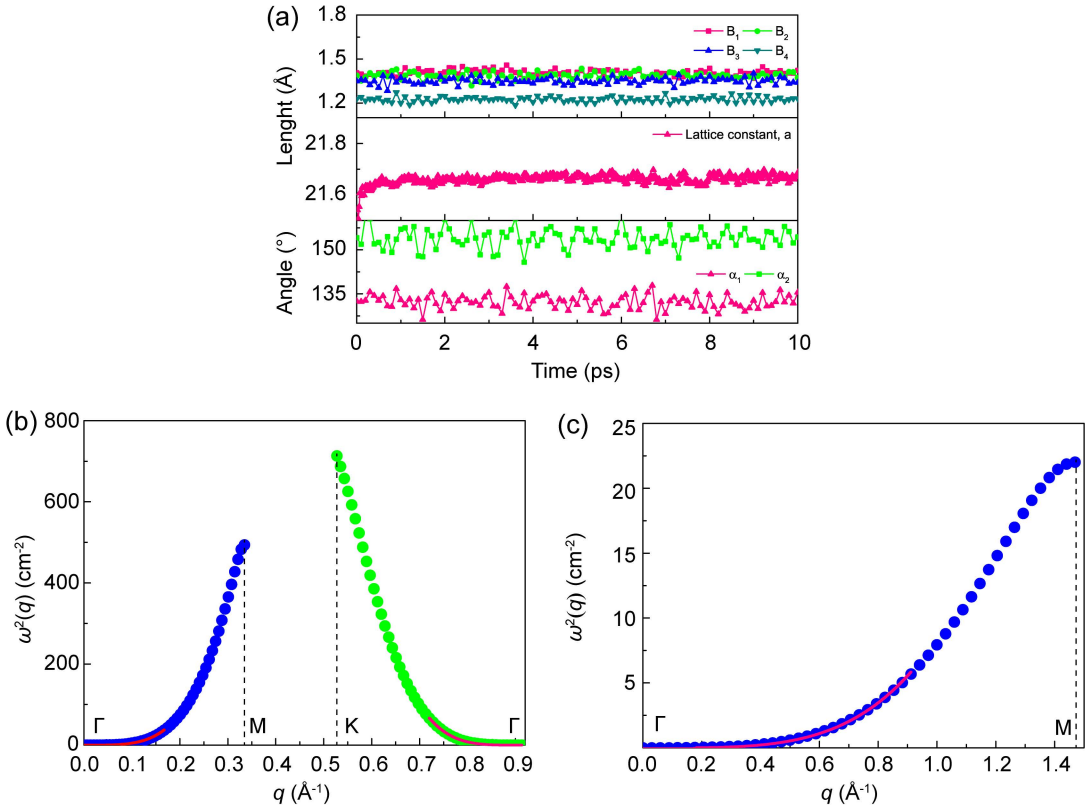

Fig. S2 (a) The fluctuation of bonds, angles and lattice constant of C_{68}-GY during the AIMD simulations. The quadratic dispersion of flexural phonon mode ZA in (b) C_{68}-GY and (c) graphene, in which the red lines denote the fitting curves.

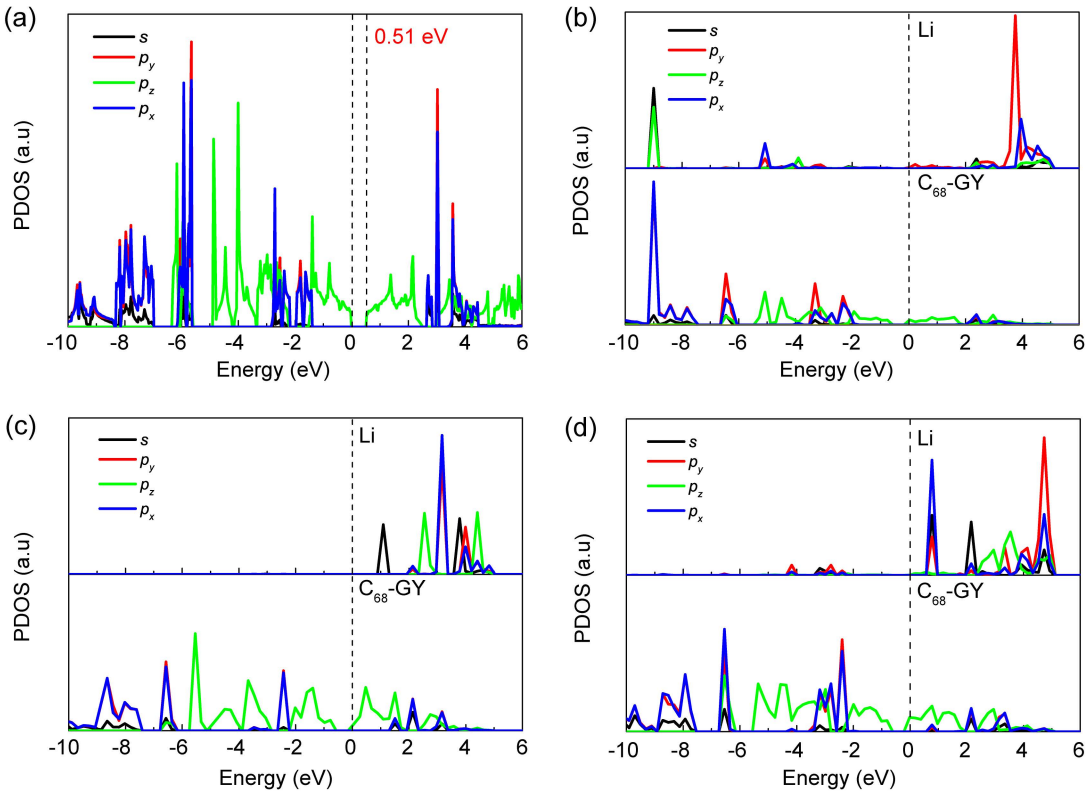

Fig. S3 Projected density of state (PDOS) of (a) pristine C_{68}-GY with an adsorbed Li on Site (b) S1, (c) S3 and (d) S4.

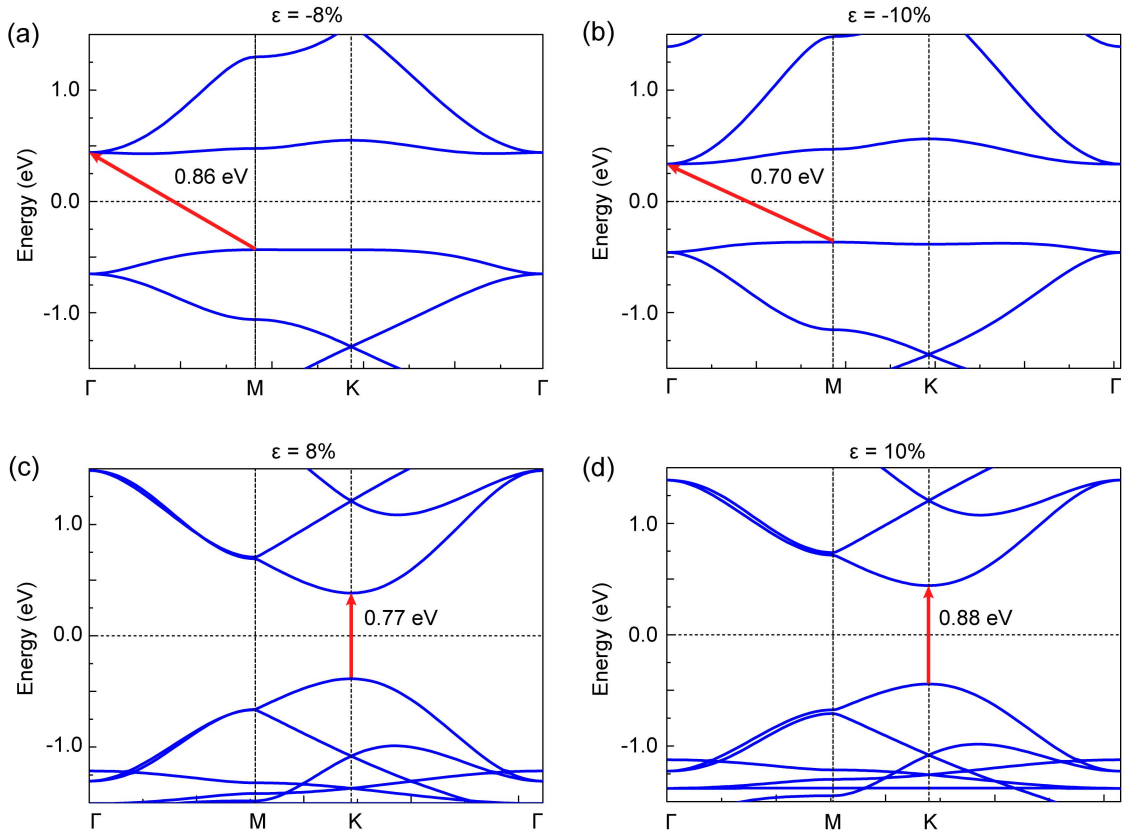

Fig. S4 Effect of biaxial strain (ε) on the band structures of C_{68}-GY.

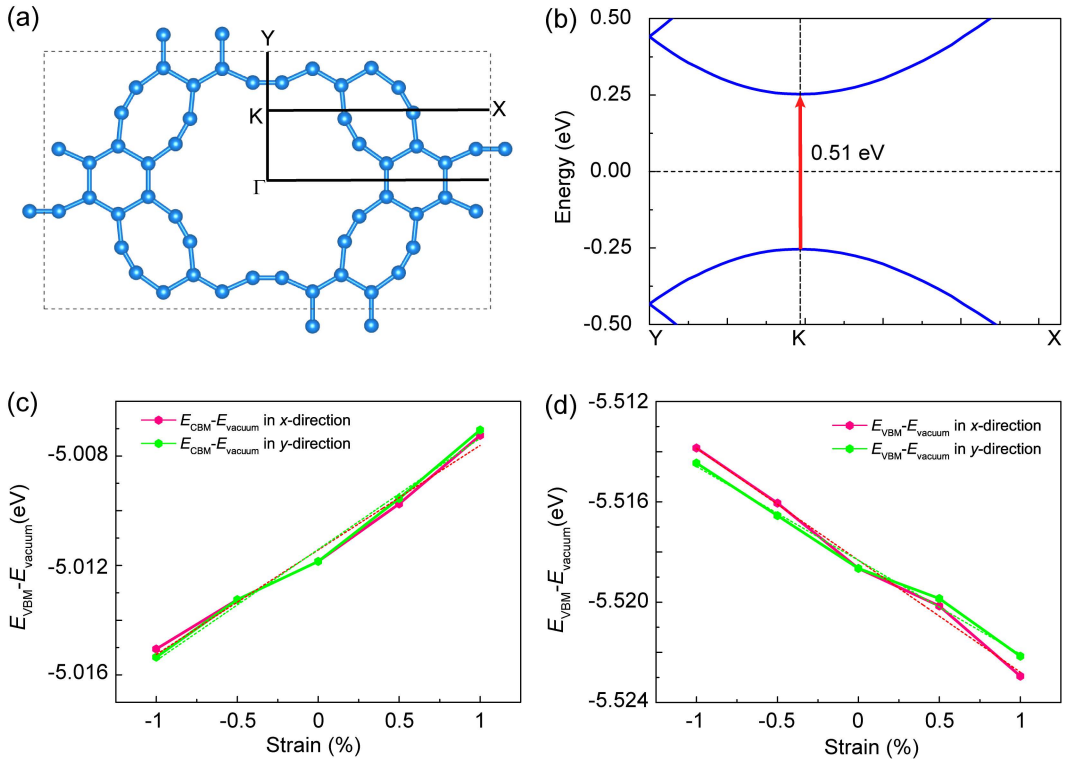

Fig. S5 (a) The K-path in the Brillouin zone for the calculation of carrier mobilities. (b) The calculated band structure along Y-K-X path at PBE functional level. Band energy shit of (c) CBM and (d) VBM under the strain along *x*- and *y*-direction. The term E_1 is determined by using $E_1=\Delta E/\varepsilon$ to fit the curves in (c) and (d). The dashed lines belong to the fitting lines with respect to *x*- and *y*-direction, respectively.

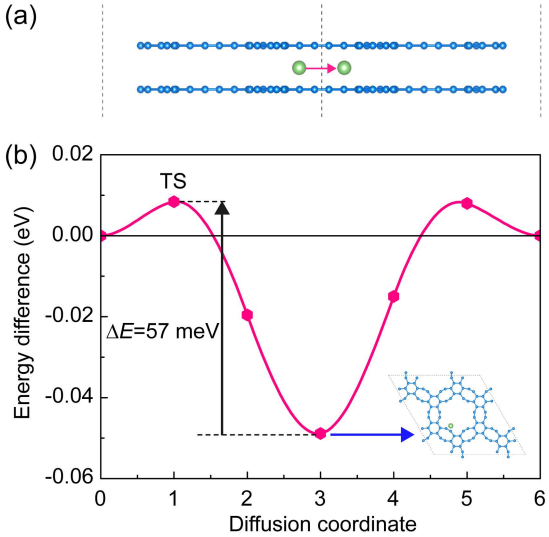

Fig. S6 (a) Schematics of the diffusion path in bilayer C_{68}-graphyne along diffusion path of P1 (side view); (b) the diffusion barrier profile.

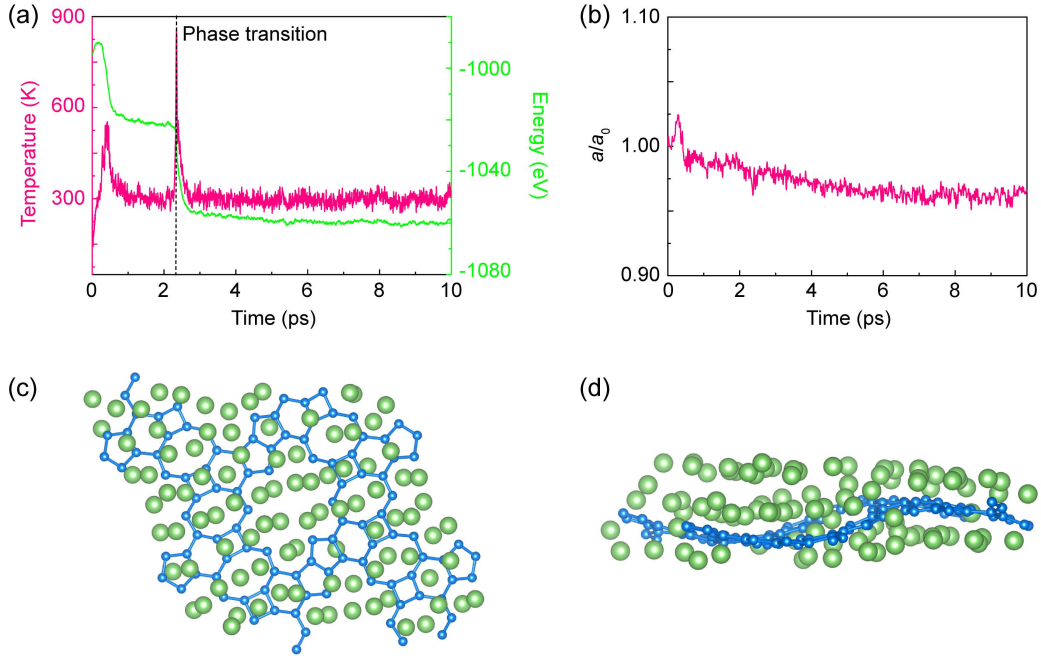

Fig. S7 The fluctuations of (a) temperature and energy in the AIMD simulations of LiC, as well as (b) the lattice changes, a/a_0; (c) Top and (d) side views of the snapshots of LiC taken from AIMD simulations. The green and blue spheres represent Li and C atoms, respectively.

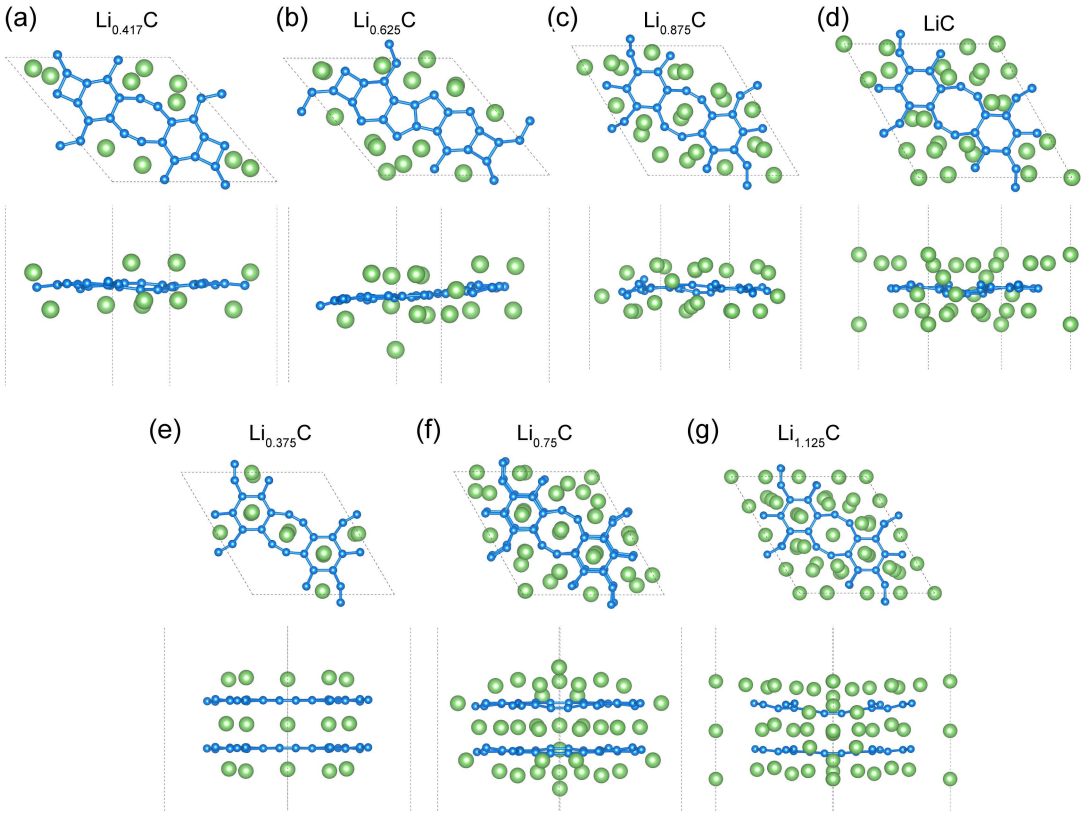

Fig. S8 (a-d) Top and side views of the intermediate configurations with different Li ion concentrations along the minimum formation energy path. (e-g) The considered configurations with varying Li concentrations intercalated in bilayer C_{68}-GY.

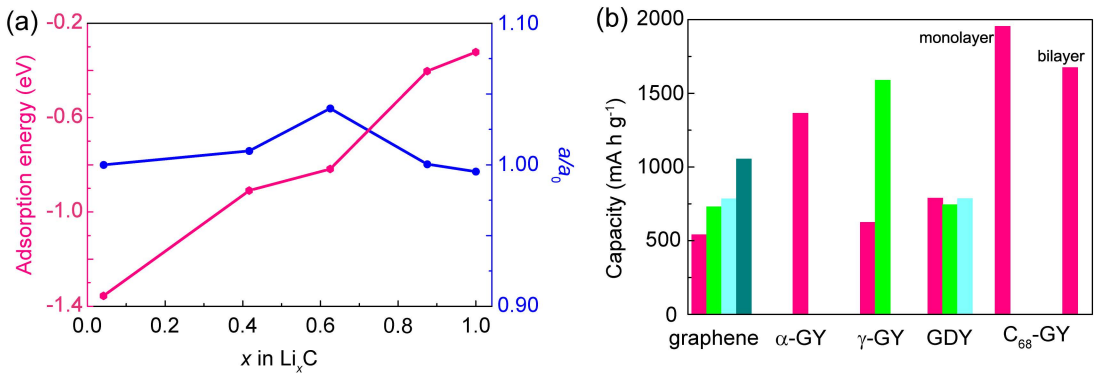

Fig. S9 (a) The calculated adsorption energy and lattice change profiles along the minimum energy path of formation energies as shown as green points in **Fig. 6a**; (b) The specific capacity (*C*) of C_{68}-GY as anode materials for LIBs, and the comparison with other typical carbon allotropes. The data for graphene, α-GY, γ-GY and GDY are obtained from **Refs. 1-7**.

Table S1 The calculated in-plane stiffness S, Poisson ratio v, tensile strengths σ_s and strain to failure ε_s of C_{68}-GY, and the comparison with other typical carbon allotropes.

Materials	S (N m^{-1})		v		σ_s (N m^{-1})		ε_s		D (eV)
	S_x	S_y	v_x	v_y	σ_{sx}	σ_{sy}	ε_{sx}	ε_{sy}	
C_{68}-GY	49.4	51.7	0.713	0.714	21.7	14.7	0.32	0.20	0.50
Graphene	350[8]	350[8]	0.186[8]	0.186[8]	36.7[8]	40.4[8]	0.194[8]	0.266[8]	1.44~1.46[9, 10]
α-GY	21.98[11]	21.98[11]	0.87[11]	0.87[11]	12.4[12]	11.0[12]	0.178[12]	0.156[12]	-
β-GY	73.07[11]	73.07[11]	0.67[11]	0.67[11]	15.7[12]	12.9[12]	0.162[12]	0.130[12]	-
γ-GY	162[13]	162[13]	0.429[13]	0.429[13]	15.4[14]	34.4[14]	0.08[14]	0.13[14]	2.69[14]
GDY	123.1[15]	123.1[15]	0.446[15]	0.446[15]	-	-	-	-	-
Graph-3-yne	101.8[15]	101.8[15]	0.436[15]	0.436[15]	-	-	-	-	-
Graph-4-yne	87.7[15]	87.7[15]	0.432[15]	0.432[15]	-	-	-	-	-

Table S2 The calculated effective masses for electrons (m_e^*) and holes (m_h^*) in the direct band structures of C_{68}-GY at PBE level with applying various biaxial strain.

Biaxial strain (%)	m_e^* / m_0 (K-M)	m_e^* / m_0 (K-Γ)	m_h^* / m_0 (K-M)	m_h^* / m_0 (K-Γ)
-6	0.641	0.298	-0.575	-0.296
-4	0.556	0.278	-0.685	-0.293
-2	0.712	0.271	-0.864	-0.294
-1	0.325	0.199	-0.342	-0.209
-0.5	0.325	0.199	-0.343	-0.210
0	0.326	0.200	-0.345	-0.211
0.5	0.326	0.200	-0.347	-0.212
1	0.327	0.201	-0.350	-0.214
2	0.329	0.203	-0.355	-0.218
4	0.336	0.210	-0.368	-0.228
6	0.347	0.221	-0.386	-0.243
8	0.364	0.238	-0.410	-0.265
10	0.391	0.266	-0.448	-0.300

References

1. E. Yoo, J. Kim, E. Hosono, H.-s. Zhou, T. Kudo and I. Honma, *Nano letters*, 2008, **8**, 2277-2282.
2. D. Pan, S. Wang, B. Zhao, M. Wu, H. Zhang, Y. Wang and Z. Jiao, *Chemistry of Materials*, 2009, **21**, 3136-3142.
3. H. J. Hwang, J. Koo, M. Park, N. Park, Y. Kwon and H. Lee, *The Journal of Physical Chemistry C*, 2013, **117**, 6919-6923.
4. K. Srinivasu and S. K. Ghosh, *The Journal of Physical Chemistry C*, 2012, **116**, 5951-5956.
5. C. Sun and D. J. Searles, *The Journal of Physical Chemistry C*, 2012, **116**, 26222-26226.
6. H. Zhang, Y. Xia, H. Bu, X. Wang, M. Zhang, Y. Luo and M. Zhao, *Journal of Applied Physics*, 2013, **113**, 044309.
7. S. Zhang, H. Du, J. He, C. Huang, H. Liu, G. Cui, Y. and Y. Li, *ACS Applied Materials & Interfaces*, 2016, **8**, 8467-8473.
8. F. Liu, P. Ming and J. Li, *Physical Review B*, 2007, **76**, 064120.
9. K. N. Kudin, G. E. Scuseria and B. I. Yakobson, *Physical Review B*, 2001, **64**, 235406.
10. Y. Wei, B. Wang, J. Wu, R. Yang and M. L. Dunn, *Nano Letters*, 2013, **13**, 26-30.
11. A. R. Puigdollers, G. Alonso and P. J. C. Gamallo, *Carbon*, 2016, **96**, 879-887.
12. Y. Zhang, Q. Pei and C. Wang, *Applied Physics Letters*, 2012, **101**, 081909.
13. Q. Peng, W. Ji and S. De, *Physical Chemistry Chemical Physics*, 2012, **14**, 13385-13391.
14. S. W. Cranford and M. J. Buehler, *Carbon*, 2011, **49**, 4111-4121.
15. Q. Yue, S. Chang, J. Kang, S. Qin and J. Li, *The Journal of Physical Chemistry C*, 2013, **117**, 14804-14811.